

Monitoring H-cluster assembly using semi-synthetic HydF

Brigitta Németh, Charlène Esmieu, Holly J. Redman and Gustav Berggren

Supporting information

Table of Contents

Figure S1. The effect of the baseline treatment on the FTIR spectra.

Figure S2. Hemoglobin calibration curves.

Figure S3. UV/Vis and EPR spectra recorded on CrHydA1 and CaHydF after reconstitution.

Figure S4. Monitoring $[2\text{Fe}]^{\text{adt}}$ -HydF formation by UV/Vis spectroscopy.

Figure S5. Monitoring the reaction between $[2\text{Fe}]^{\text{adt}}$ and thionine by UV/Visible spectroscopy.

Figure S6. Quantification of HydF reduction during H-cluster assembly using EPR spectroscopy.

Figure S7. Monitoring H-cluster assembly over time by EPR spectroscopy.

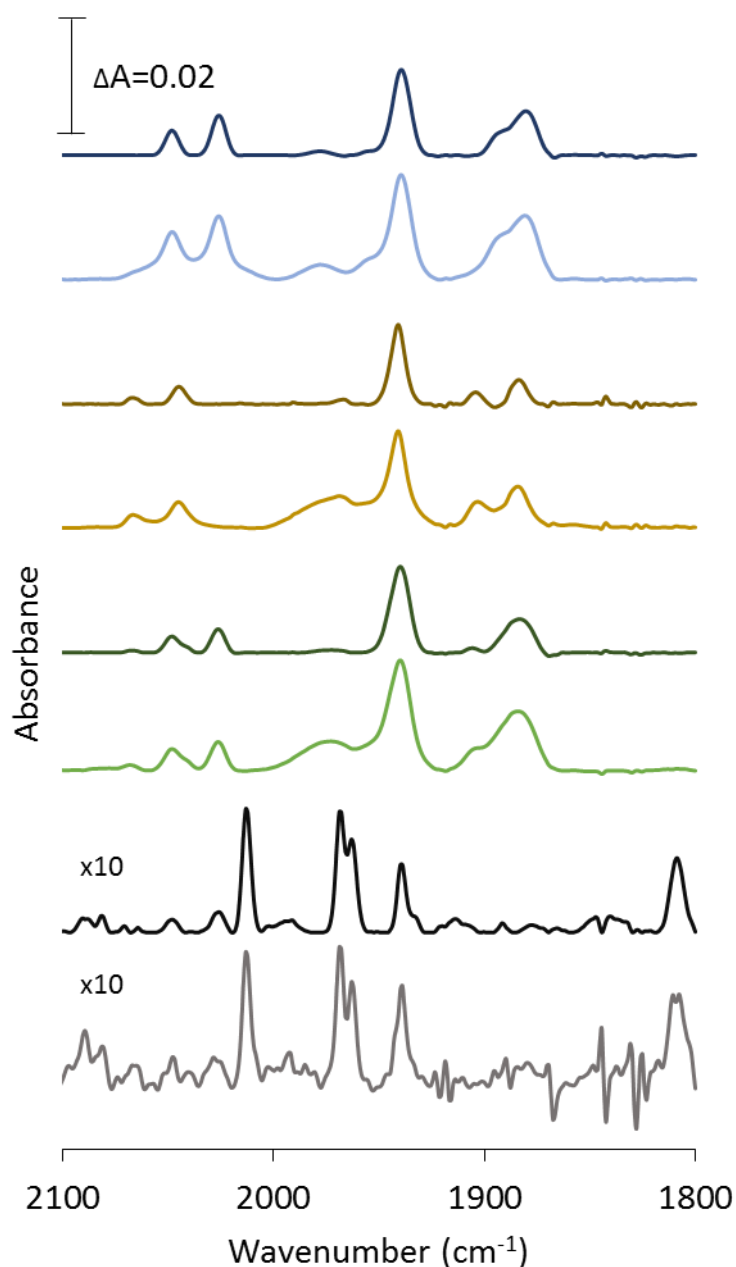


Figure S1. The effect of the baseline treatment on the FTIR spectra.

The rubber-band concave (RBC) baseline treatment was carried out in OPUS (Bruker), the manual polynomial (MP) baseline treatment was carried out in Origin. From top to bottom: $[2\text{Fe}]^{\text{adt}}\text{-CaHydF}$ as prepared RBC (dark blue), $[2\text{Fe}]^{\text{adt}}\text{-CaHydF}$ as prepared MP (light blue); $[2\text{Fe}]^{\text{adt}}\text{-CaHydF}$ thionine acetate oxidized RBC (dark yellow), $[2\text{Fe}]^{\text{adt}}\text{-CaHydF}$ thionine acetate oxidized MP (light yellow); $[2\text{Fe}]^{\text{adt}}\text{-CaHydF}$ Na-DT reduced RBC (dark green), $[2\text{Fe}]^{\text{adt}}\text{-CaHydF}$ Na-DT reduced MP (light green); $[2\text{Fe}]^{\text{adt}}\text{-CaHydF} + \text{apo-CrHydA1}$ RBC (black), $[2\text{Fe}]^{\text{adt}}\text{-CaHydF} + \text{apo-CrHydA1}$ as prepared MP (black). The two baseline treatment protocols result in limited changes to relative peak intensities and the peak shape, while peak position remain constant. Sample conditions are given in Figure 2 and 4 of the main text. Due to low sample concentration and signal intensity, the two latter spectra were multiplied by the factor of 10.

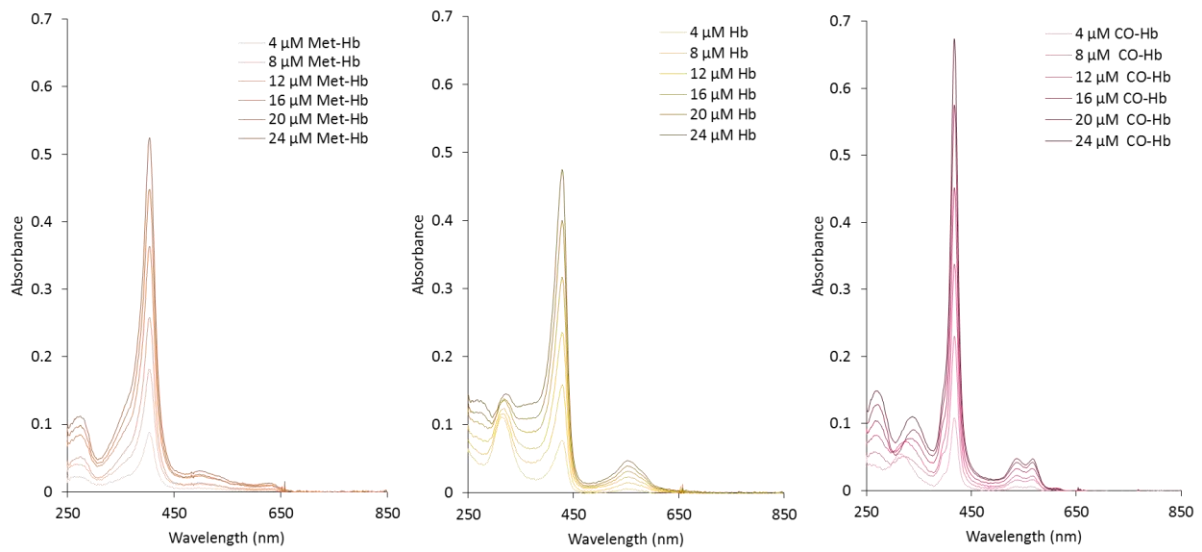


Figure S2. Hemoglobin calibration curves. Methemoglobin, deoxyhemoglobin (Hb) and carboxyhemoglobin (CO-Hb) calibration curves. 100 μM met-hemoglobin solution was prepared from bovine hemoglobin (Sigma) dissolved in 100 mM K-phosphate buffer pH 6.8. Dilution curve was prepared in the range of 1-6 μM hemoglobin concentrations in 100 mM K-phosphate buffer pH 6.8. Each methemoglobin sample was measured by UV/Vis (hemoglobin ox). Deoxyhemoglobin was generated via the addition of 100 μM (final concentration) of Na-DT to each methemoglobin sample. After a 5 minute incubation period the UV/Vis spectrum was recorded for each sample (hemoglobin red). To obtain the carboxyhemoglobin form, the deoxyhemoglobin samples were transferred into gas tight serum vials and flushed with pure CO gas for 5 minutes. The vials were opened in the glovebox and their respective UV/Vis spectra were recorded (hemoglobin CO). The spectra were recorded with a $l=0.2$ cm cuvette.

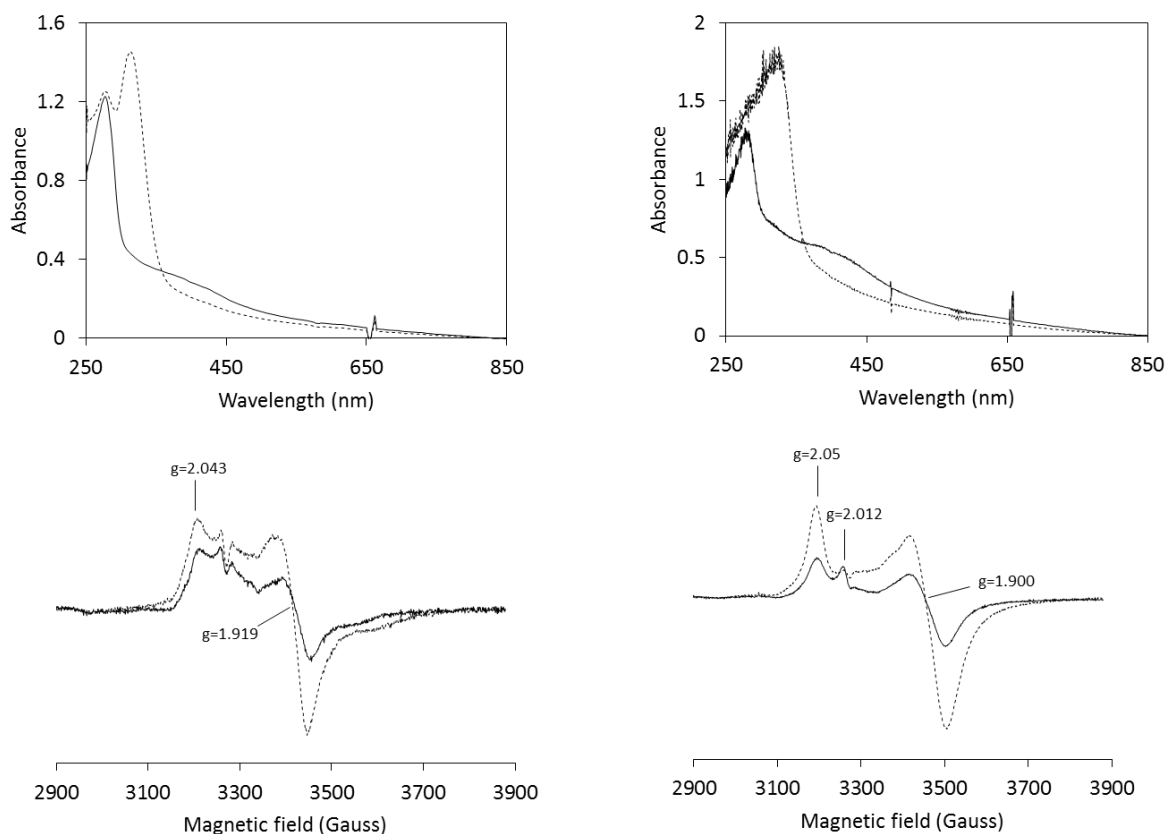


Figure S3. UV/Vis and EPR spectra recorded on CrHydA1 and CaHydF after reconstitution. Left panel: (top) UV/Vis spectra of CrHydA1 (100 μM) after reconstitution in the absence (black solid line) or presence of dithionite (2 mM, black dashed line); (bottom) EPR spectra of CrHydA1 (200 μM) in the absence (black solid line) or presence of dithionite (4 mM, black dashed line). Right panel: (top) UV/Vis spectra of CaHydF (200 μM) after reconstitution in the absence (black solid line) or presence of dithionite (2 mM, black dashed line); (bottom) EPR spectra of CaHydF (200 μM) in the absence (black solid line) or presence of dithionite (2 mM, black dashed line). EPR spectra recorded at 10K, microwave power 1 mW. Microwave frequency: 9.28 GHz. All samples were prepared in 100 mM Tris-HCl 300 mM KCl 25 mM MgCl_2 buffer. The spectra were recorded with a $l=0.2$ cm cuvette.

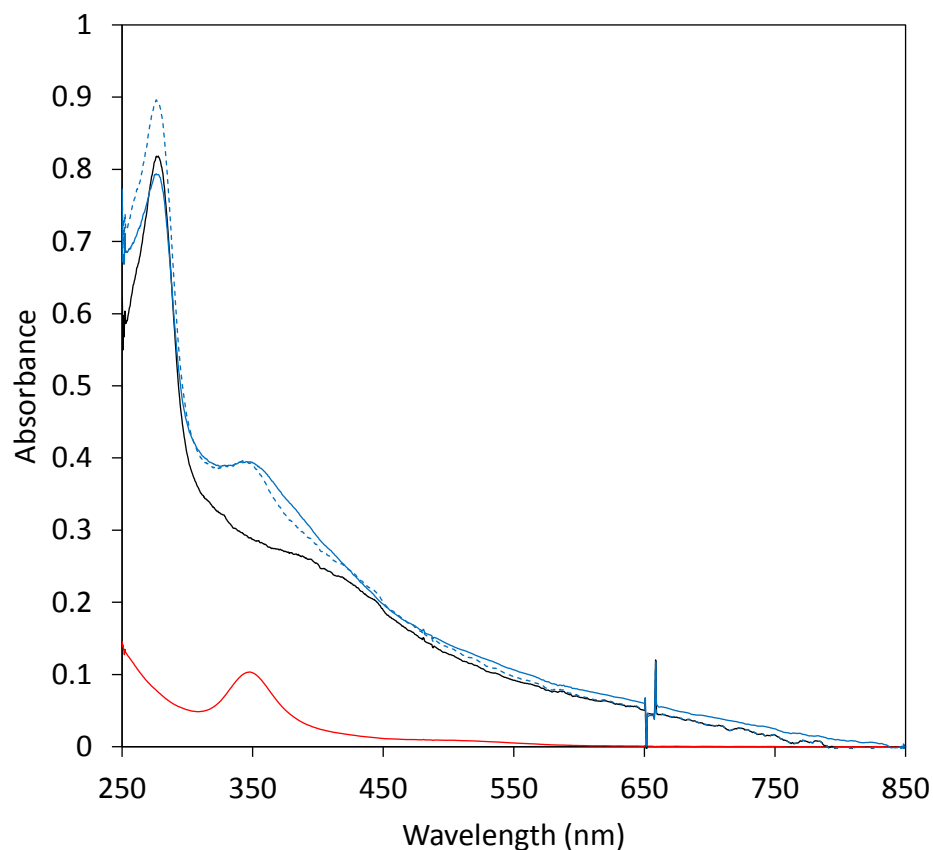


Figure S4. Monitoring $[2\text{Fe}]^{\text{adt}}\text{-HydF}$ formation by UV/Vis spectroscopy. The solid lines represent experimental data, while the dashed line represent a linear combination of two experimental spectra. $130\ \mu\text{M}$ $[\text{4Fe}_4\text{S}]^{2+}\text{-CaHydF}$ (solid black), $130\ \mu\text{M}$ $[2\text{Fe}]^{\text{adt}}\text{-CaHydF}$ (solid blue line); $130\ \mu\text{M}$ $[2\text{Fe}]^{\text{adt}}$ (solid red); A linear combination of $130\ \mu\text{M}$ $[2\text{Fe}]^{\text{adt}}$ and $130\ \mu\text{M}$ $[\text{4Fe}_4\text{S}]^{2+}\text{-CaHydF}$ spectrum (dashed blue). All spectra were recorded in $100\ \text{mM}$ Tris-HCl pH 8.0, $300\ \text{mM}$ KCl. The spectra were recorded with a $l=0.2\ \text{cm}$ cuvette.

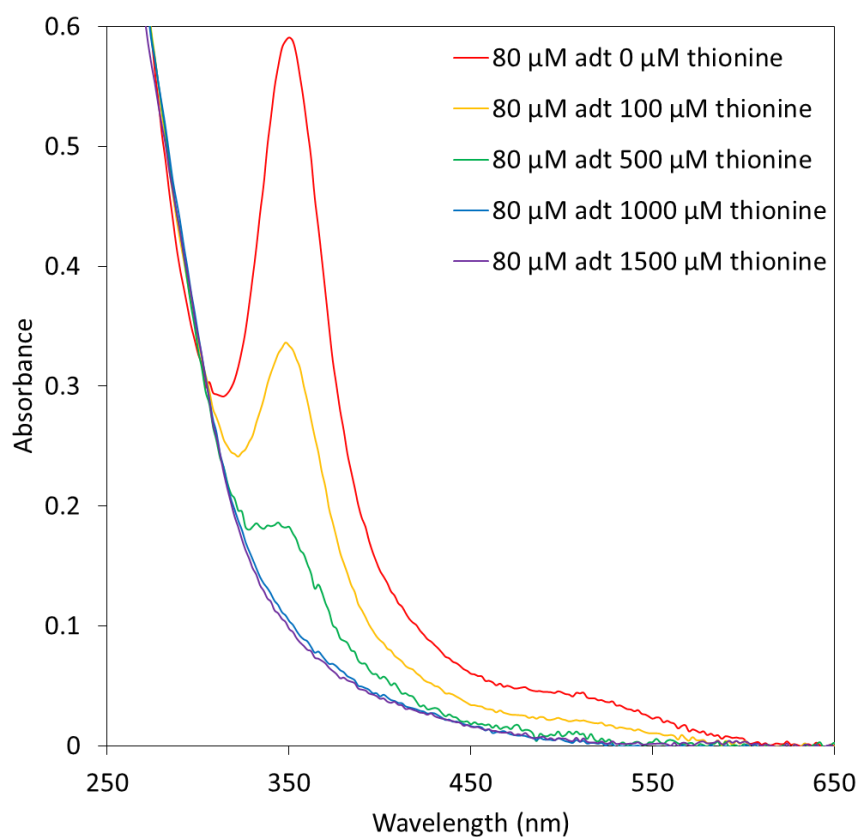


Figure S5. Monitoring the reaction between $[2\text{Fe}]^{\text{adt}}$ and thionine by UV/Visible spectroscopy. 80 μM $[2\text{Fe}]^{\text{adt}}$ complex was treated with various amounts (100-1500 μM , 1.25-18.75 equivalents) of thionine acetate for 5 minutes under strict anaerobic conditions in the glovebox at room temperature under dimmed light conditions, resulting the disappearance of the characteristic absorption band at 350 nm. The $[2\text{Fe}]^{\text{adt}}$ complex was dissolved in 100 mM Tris-HCl pH 8.0, 300 mM KCl, 25 mM MgCl_2 . The solid thionine acetate powder was dissolved in 100 mM Tris-HCl pH 8.0, 300 mM KCl, 25 mM MgCl_2 . The excess solid thionine acetate particles were removed via filtration before recording the UV/Vis spectra. The spectra were recorded with a $l=1$ cm cuvette.

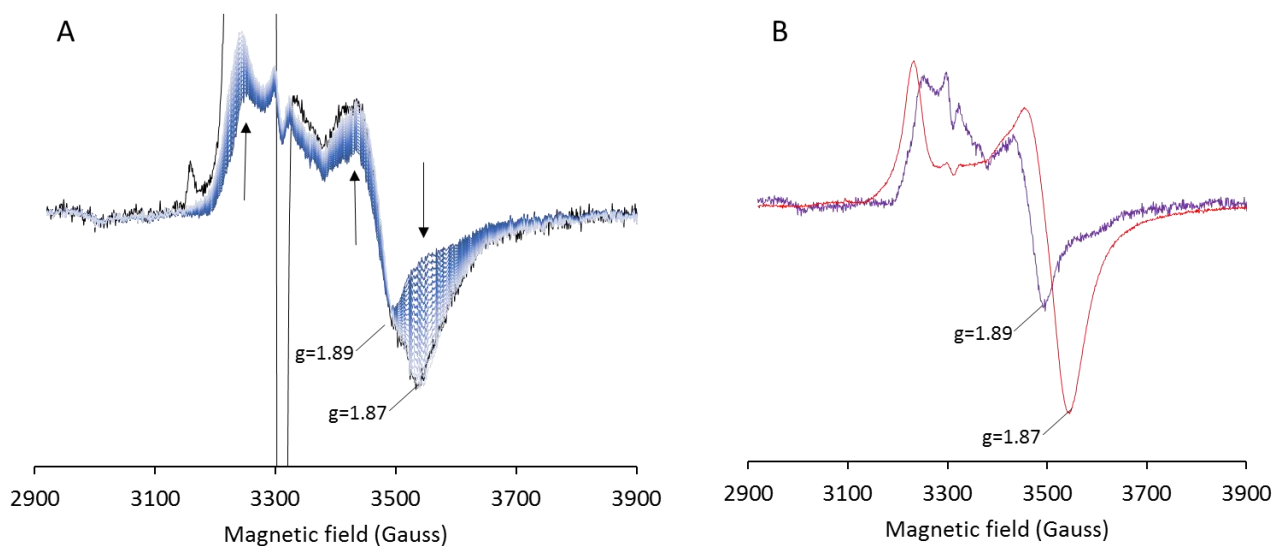


Figure S6. Quantification of HydF reduction during H-cluster assembly using EPR spectroscopy. Panel A: Low temperature X-band EPR spectrum recorded on a mixture of 200 μM CrHydA1 and 30 μM $[\text{2Fe}]^{\text{adt}}\text{-CaHydF}$ incubated for 60 minutes, recorded at 10 K with 1 mW microwave power, microwave frequency: 9.28 GHz. (black solid line); and a reproduction of the experimental spectrum through a linear combination of CrHydA1 (as-prepared, 200 μM) and increasing concentrations (1 μM -16 μM , shown as dark to pale blue) of reduced CaHydF ($[\text{4Fe4S}]^+\text{-CaHydF}$). The H_{ox} and $\text{H}_{\text{ox-CO}}$ signals observable at $g \geq 2$ are not included in the fitting.

Panel B: Representative spectra of $[\text{4Fe4S}]^+\text{-CrHydA1}$ (as-prepared, 200 μM) (purple solid line) and 30 μM dithionite treated CaHydF ($[\text{4Fe4S}]^+\text{-CaHydF}$, red solid line) used in the fitting procedure shown in panel A. Troughs at $g = 1.89$ ($[\text{4Fe4S}]^+\text{-CrHydA1}$) and 1.87 ($[\text{4Fe4S}]^+\text{-CaHydF}$) indicated for clarity.

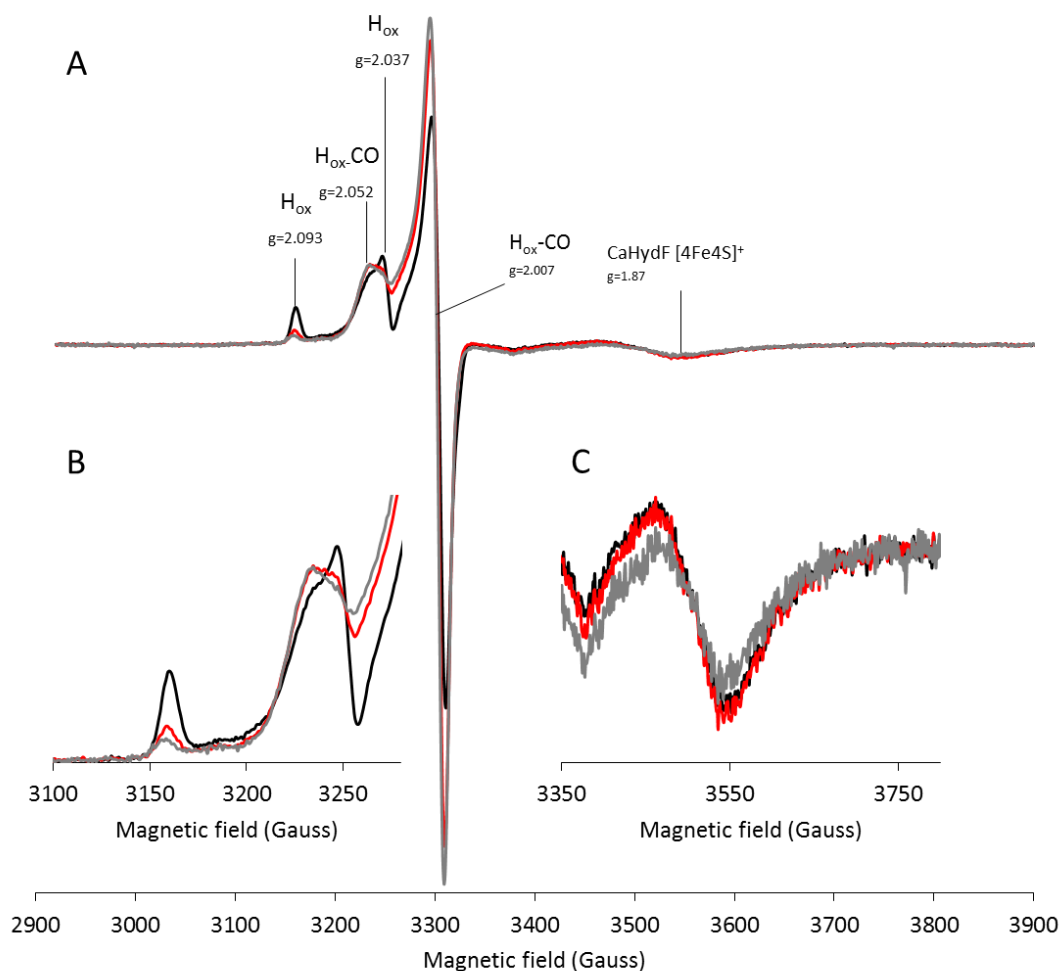


Figure S7. Monitoring H-cluster assembly over time by EPR spectroscopy. A mixture of apo-CrHydA1 (200 μ M) and $[2\text{Fe}]^{\text{adt}}\text{-CaHydF}$ (30 μ M) was prepared under anaerobic conditions, and EPR samples collected after 6 (black spectrum), 16 (red spectrum) and 60 (grey spectrum) minutes were flash frozen in liquid nitrogen. There is an increase in the H_{ox} signature observable between the 6 and 16 minute spectra, with a concomitant decrease of the $\text{H}_{\text{ox-CO}}$ features. Extended incubation times (60 minutes spectrum) transforms the majority of the sample back into $\text{H}_{\text{ox-CO}}$. Panel A: Full scan window, highlighting changes in the intense $\text{H}_{\text{ox-CO}}$ feature at $g = 2.007$; Panel B: Zoom in of low field region (3100-3300 Gauss), highlighting changes in the characteristic peak of H_{ox} at $g = 2.10$; Panel C: Zoom in of high field region (3350-3650 Gauss), highlighting changes in the $g = 1.87$ signal attributed to $[\text{4Fe4S}]^+\text{-CaHydF}$. HydF becomes reduced within minutes, and only minor changes are observed upon extended incubation.

Spectra were recorded at recorded at 10 K with 1 mW microwave power, microwave frequency: 9.28 GHz.